Energy Savings for Virtual MISO in Fractal Sensor Networks

Milan Bradonjic, Philippe Jacquet, Dalia Popescu

Energy Savings for Virtual MISO in Fractal Sensor Networks

Milan Bradonjić[1] , Philippe Jacquet[2] and Dalia Popescu[2]
[1]Rutgers University, [2]Nokia Bell Labs
dalia.popescu15@gmail.com, philippe.jacquet@nokia-bell-labs.com

***Abstract*—We design a model of wireless terminals, i.e. transmitters and receivers, obtained from a Poisson point process with support in an embedded fractal map. The terminals form a virtual MISO (Multiple Input Single Output) system with successful reception under SNR (signal-to-noise ratio) capture condition in a single hop transmission. We show that if we omit antennas cross sections, the energy needed to broadcast a packet of information tends to zero when the density of transmitters and receivers increases. This property is a direct consequence of the fact that the support map is fractal and would not hold if the terminal distribution were Poisson uniform, as confirmed by simulations. The result becomes invalid if the cross sections overlap or if we consider a masking effect due to antennas, which would imply an extremely large density of terminals. In the case where the cross sections of the transmitters have a non-zero value, the energy has a non-zero limit which decays to zero when the cross sections tend to zero.**

I. Introduction

Sensors, the major electronic elements that constitute a sensor network, are devices of a limited size that dispose of a limited amount of energy. To optimize the energy consumption, one important role is given by constraints to the topology of the networks, as geometry arises as a major factor in the determination of the transmission powers.

One of commonly used stochastic assumptions in the theoretical studies of wireless networks is that nodes of a network, at any given time, are represented as a realization of a two-dimensional (planar) Poisson point process (PPP). There has been a large body of work focused on the understanding of the fundamental properties of wireless networks under the assumption of a planar PPP [1]–[4]. In general, sensors or mobile nodes are not randomly placed over a plane. They rather follow geometric patterns with a certain level of regularity defined by a network design plan itself, as well as sometimes by repulsion properties [5], etc.

A recently considered concept for modeling wireless networks is self-similarity. For example, the world has a certain degree of self-similarity that can be easily observed in organizational structures such as urban environment [6], [7]. In more details: (i) towns are split in neighborhoods and quarters, where each neighborhood is organized in blocks separated by streets; (ii) blocks are made of buildings that are themselves split in apartments, where each apartment is made of rooms; (iii) the space of each room is delimited again by furniture pieces; and so on. Unavoidably, networks inherit a part of the environment structure. Patterns, symmetry and further more, self-similarity have been proven to be captured successfully by fractal models. These models have been proven to show better performances than two-dimensional PPP based models [6].

This work addresses the case of a network of sensors (transmitters and receivers) that are distributed according to a model of fractal repartition. The sensors follow a virtual MISO communication setup, namely, the synchronized transmitters broadcast the same packet to a set of receivers in a single transmission. We present results on the total energy consumption for correct packet reception: the energy decays towards zero when the density of population increases considerably, under specific assumptions. Furthermore, by getting closer to a fractal repartition of nodes, a sensor network spends less and less energy.

This zero energy limit is a property which is a direct consequence of the fact that the sensor networks lays in a fractal map, and should not hold if the terminal distribution is Poisson homogeneous. Anyhow we believe that this property should extend to self similar maps other than fractal maps. The validity of the following results is based on the assumption of non-overlapping antenna cross section. However the assumption fails only when assuming an overwhelming density of terminals such that antennas get into contact of each other.

When the cross section of the transmitters has a non-zero value, the energy has a non-zero limit. By further allowing the cross section to go to zero, this limiting energy decays to zero as well. Furthermore, in the analysis we neglect the masking effect between antennas and therefore the energy received by one antenna can be reused by another one. This assumption holds as the cumulated quantity of energy captured by the antennas is extremely small.

Sensors usually have antennas physically larger than a half-wavelength of the radiation they emit. These antennas have three operating regions: near-field, Fresnel zone and far-field [8]. Far-field region is the region where one can use Rayleigh fading to characterize the effects of the propagation. The condition for being in far field is to be located at least at the Fraunhofer distance $d = (2D^2)/\lambda$ where D is the antenna diameter and λ the wavelength [8]. E.g. For some typical values for sensor networks as the antenna diameter 1cm and operating frequency at 2.4GHz, the far-field starts at about 1.633cm away from the antenna, therefore even in random placement, antenna cross section overlapping has a very low probability proportional to d^2 over the expected area of the

Work was peformed at Nokia Bell Labs.

network map (few squared kilometers).

A. Related work

Here we detail some of the recent results. The topology and performance evaluation of sensor networks have been largely debated in the scientific literature [9]. While [1] gives well-known results in two network scenarios, one including arbitrarily located nodes and traffic patterns and the other one with randomly located nodes and traffic patterns, [10] studies the performance over time obtained in the tree-like sensor networks. [11] gives an analytical approach for modeling the coverage and connectivity of sensor grids as functions of key parameters such as the number of nodes and their transmission radius.

Authors of [12] investigate capacity in virtual MISO networks modeled using a uniform point process. In [13], capacity is evaluated in MISO setups, exploiting fractal maps, namely, when several simultaneous emitters of different and independent data and a single access point are randomly distributed in an infinite fractal map embedded in a space of finite dimension. Other works target computing the energy requirements in the case when multi hop scenario is deployed [14].

However, this paper addresses the issues where the emitters transmit the same data and the capture condition must be fulfilled in a **single transmission**. Furthermore, by using fractal geometry, we show that in such a modeling of the sensors networks, significant energy saving can be obtained, much superior to previously used models.

The remainder of the paper is organized as follows. In Section II we present the model. Sections III and IV provide our main theoretical results and the corresponding proofs. In Section V, we present the simulation experiments that exhibit the performance of the proposed topologies comparing them to the performance obtained in classic topologies (e.g. Poisson point processes). We conclude and suggest further research in section VI.

II. Model Description

We consider the network map embedded in the unit square $[0,1]^2$ where the distributions of transmitters and receivers follow the fractal distribution as it will be detailed in the next section.

Let $\mathcal{T}$ be the set of transmitter positions and $\mathcal{R}$ the set of receiver positions. The number of elements in $\mathcal{R}$ is n and the number of elements in $\mathcal{T}$ is a Poisson random variable of mean λ_n. Furthermore, we consider $\lambda_n = O(n)$, since one of our main goals is to analyze a communication when the number of transmitters is not bigger than the number of receivers.

Each transmitting node uses the same nominal transmit power, P_n. The power can evolve as a function in n when the setting parameters of the problem vary. The signal power path-loss is modeled by a function $l(r) = (Ar)^\alpha$ where A is a constant, r is the distance between the transmitter and the receiver and $\alpha \geq 2$ is the attenuation factor that characterizes the environment in which the devices communicate.The model comprises also the aperture of the receiver antenna, δ which becomes small when the antenna cross sections decay [15] as we will see after. For every pair $\mathbf{x} \in \mathcal{T}$ and $\mathbf{y} \in \mathcal{R}$ at denote by $S_n(\mathbf{x}, \mathbf{y})$ a signal received at $\mathbf{y}$ from $\mathbf{x}$:

$$S(\mathbf{y}, \mathbf{x}) = \delta P_n \|\mathbf{y} - \mathbf{x}\|^{-\alpha}, \tag{1}$$

Throughout this work, we refer to the case when $\alpha = 2$ which is the attenuation factor in vacuum. This an assumption that holds in our scenario, as in a high density of receivers and transmitters, the greatest contribution in the received energy at a certain node $\mathbf{y}$ comes from transmitters that are located at very small distances from $\mathbf{y}$ such that the signal hardly suffers any attenuation due to the environment.

To avoid a singular behavior, a more realistic hypothesis is to assume that a signal received at $\mathbf{y}$ from $\mathbf{x}$ is

$$S_n(\mathbf{y}, \mathbf{x}) = \delta P_n \left(\max\{d_{\min}, \|\mathbf{y} - \mathbf{x}\|\}\right)^{-\alpha}, \tag{2}$$

where $d_{\min}$ is typically of the order of the width of the antennas of both devices. In fact δ should contain a factor of order $d_{\min}^{\alpha-2}$ due to the fact that the quantity of energy radiated through the antenna cross section remains constant when $d_{\min} \to 0$, but this factor disappears if we consider $\alpha = 2$.

Signal-power is also perturbed by random fading $\mathbf{F}$, independently sampled for each transmitter-receiver pair at each time slot. A signal received at receiver at position $\mathbf{y}$ from transmitter at position $\mathbf{x}$ can have a random (multiplicative) fading factor $\mathbf{F}(\mathbf{x}, \mathbf{y})$, which modifies the received power as:

$$S_n(\mathbf{y}, \mathbf{x}) = \delta \mathbf{F}(\mathbf{x}, \mathbf{y}) P_n \left(\max\{d_{\min}, \|Y_r - X_t\|\}\right)^{-\alpha}. \tag{3}$$

In this paper we will restrict to an important special case where $\mathbf{F}(.)$ is exponentially distributed, which corresponds to the situation of independent non selective Rayleigh fading with $\mathbb{P}\{\mathbf{F}(\mathbf{x}, \mathbf{y}) > x\} = e^{-x}$.

The offset entropy is the entropy created by the channel due to the packet transmission starting times, differences in delays in the transmission circuits, etc. To get the capacity of the channel, one should remove the offset entropy from the entropy received. In this work, we assume a large volume of information per packet and that the offset entropy reported per symbol is negligible.

The transmission is done by broadcast. All the transmitters send identical packets to all the receivers. We are interested in the received energy at each receiver, therefore we shall name our setup a "virtual MISO setup" ,"virtual" as the transmitting antennas are geographically separated and single output as we are interested in the quantity of energy received by each receiver. Thus, the signal received at $\mathbf{y}$ denoted by $S_n(\mathbf{y}, \lambda_n)$ is equal to the sum of the received signal over all transmitters:

$$S_n(\mathbf{y}, \lambda_n) := \sum_{\mathbf{x} \in \mathcal{T}} S_n(\mathbf{y}, \mathbf{x}). \tag{4}$$

We also make use of SNR capture condition which means the following. Denote by N the noise at a node $\mathbf{y}$ and by K a non-zero level of signal strength, the threshold over which a transmission is considered successful. A packet is successfully

received by node $\mathbf{y}$ if the cumulated received signals from all the transmitters λ_n is higher than the threshold NK.

To simplify our analysis we will assume that N is proportional to the aperture δ by a constant factor which will allow us to indifferently consider δ constant or tending to zero. This would be in theory the case if the noise is limited to some external spurious signals or interferences captured by the antenna. If we consider that the noise can also be internal to the receiver, one must assume the noise decays linearly with the aperture. In the whole remainder of the paper we will just assume $N = \delta = 1$ in order to simplify the formulas.

More precisely, our goal is to find the level of energy such that all devices in $\mathcal{R}$ correctly receive the packet, in other words no node is in outage. We define the probability that a node is in outage as loss probability and we denote it by ρ_n:

$$\rho_n = \mathbb{P}\left\{\exists \mathbf{y} \in \mathcal{R} : \ S_n(\mathbf{y}, \lambda_n) < K\right\} \tag{5}$$

When taking into account the Rayleigh co-interference of the signals, we should replace $S_n(\lambda_n, \mathbf{y})$ by $\mathbf{F}(\mathbf{y})S_n(\lambda_n, \mathbf{y})$.

In this work we will assume $S_n(\mathbf{y}, \mathbf{x})$ to be governed by (1), which will lead to a simplified analysis but we will perform simulations for both cases when $S_n(\mathbf{y}, \mathbf{x})$ is governed by (1) or (2). Importantly, the effect of (2) has an impact on the results at 'extremely' high densities of the devices.

A. Fractal maps

In order to give a more clear understanding of these results, we briefly remind the fractal maps introduced in our previous work.

The Cantor maps are the support of the population of transmitters and receivers in our model. The sensor networks inherit the property of self-similarity from the cantor map.

Let us first define the binary Cantor map and more generally the ℓ-ary Cantor map, where $\ell \geq 2$ is an integer. This repeats the presentation done in [6], [13].

Definition 1 (ℓ-ary Cantor maps)**.** *Let $\ell \geq 2$ be an integer and $0 \leq a \leq 1/\ell$. The ℓ-Cantor finite map is the fractal set $\mathcal{K}(a, \ell)$ that satisfies $\mathcal{K}(a, \ell) = \cap_{k\geq 0}\mathcal{K}_k(a, \ell)$ and $\mathcal{K}_0(a, \ell) = [0, 1]$ and $\mathcal{K}_{k+1}(a, \ell) = \bigcup_{j=0}^{j=\ell-1}(j(a + b) + a\mathcal{K}_k(a, \ell))$ with $a + b = (1 - a)/(\ell - 1)$. The infinite ℓ-Cantor map $\mathcal{K}^*(a, \ell)$ satisfies $\mathcal{K}^*(a, \ell) = \cup_{k\geq 0}a^{-k}\mathcal{K}(a, \ell)$. The fractal dimension is $d_F = -\frac{\log \ell}{\log a}$.*

One can notice that the finite Cantor map is contained in the interval $[0, 1]$. The fractal dimension is obtained by observing that reducing distance by factor a gives exactly the ℓth half of the set: $a^{d_F} = 1/\ell$. The fractal dimension of $\mathcal{K}(a, \ell)^2$ embedded in $(\mathbb{R}^+)^2$ is $-2\frac{\log \ell}{\log a}$.

Definition 2 (The infinite Cantor map)**.** *The infinite Cantor map is the fractal set $\mathcal{K}^*(a)$ on $\mathbb{R}^+$ that satisfies $\mathcal{K}^*(a, \ell) = \cup_{k\geq 0}a^{-k}\mathcal{K}(a, \ell)$,*

We notice that the infinite Cantor map spans in the whole $\mathbb{R}^+$ and that $\mathcal{K}(a) = \mathcal{K}^*(a) \cap [0, 1]$.

As a demonstration of the previous definitions, Figure 1a presents the network support $\mathcal{K}^2(1/8, 4)$ and Figure 1b presents a Poisson shot on the Cantor map $\mathcal{K}^2(1/8, 4)$ The population analyzed in our model is obtained as such a Poisson shot.

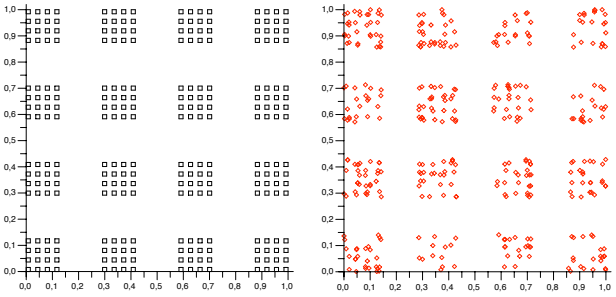

(a) The network support (b) Poisson shot on $\mathcal{K}^2(1/8, 4)$.

Furthermore, this representation of the Poisson shots on Cantor maps can be used to represent a Poisson Point Process and all the stages between a uniform Poisson Point Process and a Poisson shot on a Cantor map. Figures 2a,2b, 2c,2d illustrate four topologies obtained for different values of a and l.

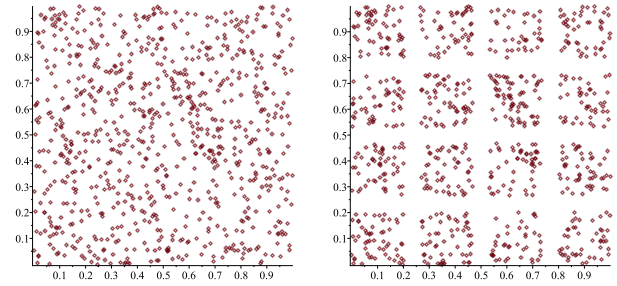

(a) $l = 4, a = 0.25$. (b) $l = 4, a = 0.2$

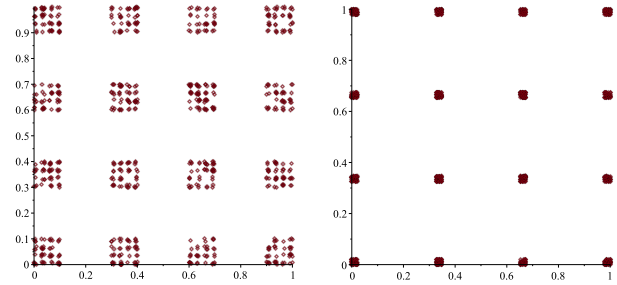

(c) $l = 4, a = 0.1$. (d) $l = 4, a = 0.02$

III. Main results

Definition 3. *We define $E_n(d)$ as the average total energy required by n receivers to ensure SNR capture when $d_{\min} = d$. We denote by $E_\infty(d) = \limsup_{n\to\infty} E_n(d)$.*

To simplify we will set $E_n = E_n(0)$. Let us now give the main results of our work.

Theorem III.1. *In a network obtained as a Poisson shot in a fractal map of dimension $d_F < 2$ where the number of*

receivers is n and the number of transmitters is a Poisson variable of mean λ_n, assuming the asymptotic case when antenna cross section is negligible, $d_{min} = 0$, and path loss coefficient is $\alpha = 2$, the loss probability, ρ_n, and the total transmitted energy required to ensure SNR capture, E_n, tend to zero, $\rho \to 0$, $\mathrm{E}_n \to 0$ when $n \to \infty$ given that:

$$\frac{\lambda_n}{\log n} \to \infty \quad (6)$$

$$\lambda_n P_n \to 0 \quad \textit{and} \quad (7)$$

$$\frac{\lambda_n P_n^{\gamma}}{(\log n)^{1-\gamma_F}} \to \infty\,, \quad (8)$$

with $\gamma_F = \frac{d_F}{\alpha}$

This theorem is the central result of our paper and states that for high densities of population of transmitters, the total energy needed to ensure packet reception decays towards zero when the density of nodes becomes overwhelming. Furthermore, the result holds because "$d_F < 2$", in other words, the phenomenon is a direct consequence of the fact that the networks is in a fractal map.

Corollary 1. *The energy required for broadcasting a packet in a virtual MISO network with n nodes in a fractal Cantor map of dimension d_F scales as:*

$$E_n = O(n^{-\beta}), \quad (9)$$

for all $\beta < \alpha/d_F - 1$.

A very important assumption for this results is $d_{min} = 0$. In the case $d_{\min} > 0$, the following holds:

Theorem III.2. *In a network obtained as a Poisson shot in a fractal map of dimension $d_F < 2$ where the number of receivers is n and the number of transmitters is a Poisson variable of mean λ_n, assuming the asymptotic case when path loss coefficient is $\alpha = 2$. Both $\rho_n \to 0$ and $E(d_{\min}) < \infty$ when n tends to infinity and $E_\infty(d_{\min}) \to 0$ when $d_{\min} \to 0$.*

IV. Theoretical proof of results

In order to prove our results, let us first compute the distribution of distance in Cantor maps.

A. Distance distribution in the Cantor map

We consider the fractal map $\mathcal{K}(a,\ell)^D$ see [6]. Let $\mu_D(Z)$ be the fractal measure on $[0,1]^D$ and define for $x \in [0,1]^D$

$$U_D(r,\mathbf{x}) := \int_{\mathbf{z}\in[0,1]^D} \mu_D(\mathbf{z}) \mathbb{I}\left(\|\mathbf{z}-\mathbf{x}\| \le r\right) d\mathbf{z}^D\,. \quad (10)$$

Then $U_D(r,\mathbf{x})$ can be seen as the distribution function of the distance from $\mathbf{z}$ to $\mathbf{x}$ with the fractal measure μ_D on $[0,1]^D$.

First, by definition from (10), we have $W_D(r,\mathbf{x}) = 0$ for all $\mathbf{x}$ when $r < 0$, and $W_D(r,\mathbf{x})$ is non-decreasing in r.

Lemma 1. *For all, r and $x \in [0,1]$ we have $U_1(r,x) \ge U_1(r,0)$.*

Proof. It is known that $\mathcal{K}(a,\ell) = \bigcap_{k\ge 0} \mathcal{K}_k(a,\ell)$. Clearly $\mathcal{K}(a,\ell) \subset \mathcal{K}_k(a,\ell)$ for all integer k and $\mathcal{K}_{k+1}(a,\ell) \subset \mathcal{K}_k(a,\ell)$. Let us define $U^k(r,x)$ as the distribution function of distances inside $\mathcal{K}_k(a,\ell)$. Clearly for all $x \in \mathcal{K}(a,\ell)$ $\lim_{k\to\infty} U^k(r,x) = U_1(r,x)$.

We want to prove that for all $x \in \mathcal{K}(a,\ell)$ and for all integer k, $U^k(r,x) \ge U^k(r,0)$.
This is true for $k = 0$ due to the following:
$U^0(r,x) \ge U^0(r,0)$ for all $x \in [0,1]$.
For all $x < 1/2$, $\quad U_1(r,x) =$
$2r\mathbb{I}\left(r \le x\right) + (x+r)\mathbb{I}\left(x < r \le 1-x\right) + \mathbb{I}\left(r > 1-x\right)$
which is greater than $U^0(r) = r$,
and $U^0(r,x) = U^0(r,1-x)$, for $x > 1/2$

For the larger values of k we proceed via induction.

Let us first take the simpler case when $0 \le x \le a$, for $k \ge 1$ one gets:

$$U^k(r,x) = \frac{1}{\ell} U^{k-1}\left(\frac{r}{a}, \frac{x}{a}\right) + \sum_{j=1}^{\ell-1} \frac{1}{\ell} U^{k-1}\left(\frac{r+x-j(a+b)}{a}, 0\right)$$

The term $\frac{1}{\ell}U^{k-1}\left(\frac{r}{a},\frac{x}{a}\right)$ describes the contribution of $\mathcal{K}_{k-1}(a,\ell)$, the division by the factor a reflects the fact that $\mathcal{K}_{k-1}(a,\ell)$ is shrunk by the factor a in the decomposition of $\mathcal{K}_k(a,\ell)$ and the factor $\frac{1}{\ell}$ reflects the fact that the set $\mathcal{K}_{k-1}(a,\ell)$ has weight $1/\ell$ in the decomposition of $\mathcal{K}_k(a,\ell)$. The term $\frac{1}{\ell}U^{k-1}\left(\frac{r+x-j(a+b)}{a}, 0\right)$ reflects the contribution of the set $j(a+b) + a\mathcal{K}_{k-1}(a,\ell)$.

Since the function $U^{k-1}(r,x)$ is non decreasing in r then the lower bound holds:

$$U^k(r,x) \ge \frac{1}{\ell} U^{k-1}\left(\frac{r}{a}, \frac{x}{a}\right) + \sum_{j=1}^{\ell-1} \frac{1}{\ell} U^{k-1}\left(\frac{r-j(a+b)}{a}, 0\right)$$

Using the recursion hypothesis that $U^{k-1}(r,x) \ge U^{k-1}(r,0)$:

$$U^k(r,x) \ge \sum_{j=0}^{\ell-1} \frac{1}{\ell} U^{k-1}\left(\frac{r-j(a+b)}{a}, 0\right) \quad (11)$$

In the left-hand side, one can recognize the term $U^k(r,0)$.

A little more delicate is the case when $x = m(a+b)+y$ with m integer greater than 0 and smaller than ℓ and $0 \le y \le a$. We further analyze it as the second and last case. The decomposition is now different since it turns out that

$$\begin{aligned} U^k(r,x) &= \frac{1}{\ell} U^{k-1}\left(\frac{r}{a}, \frac{y}{a}\right) \\ &+ \frac{1}{\ell} \sum_{j=0}^{m-2} U^{k-1}\left(\frac{r-y-b-j(a+b)}{a}, 1\right) \\ &+ \frac{1}{\ell} \sum_{j=1}^{\ell-m} U^{k-1}\left(\frac{r-y-j(a+b)}{a}, 0\right) \end{aligned}$$

The aim is still to prove that $U^k(r,x) \ge U^k(r,0)$. It is known that $U^{k-1}\left(\frac{r}{a},\frac{y}{a}\right) \ge U^{k-1}\left(\frac{r}{a},0\right)$. Notice that in the first sum in the right-hand side each term of the form $r - yb - j(a+b) = r + a - y - (j+1)(a+b) \ge r - (j+1)(a+b)$ which, in turn, is smaller than $r - (\ell - m + 1 + j)(a+b)$.

By symmetry $U^{k-1}\left(\frac{r-(\ell-m+1+j)(a+b)}{a},1\right) = U^{k-1}\left(\frac{r-(\ell-m+1+j)(a+b)}{a},0\right)$. Collecting with the terms of the second sum we obtain:

$$U^k(r,x) \geq \frac{1}{\ell}\sum_{j=0}^{m-1} U^{k-1}\left(\frac{r-j(a+b)}{a},0\right) = U^k(r,0), \tag{12}$$

which terminates the proof. □

In a higher dimension D an analogous bound is achieved:

Lemma 2. *$U_D(r,\mathbf{x}) \geq U_D(r,0)$ for all $\mathbf{x} \in [0,1]^D$.*

Proof. Denote $\mathbf{z} = (\underline{\mathbf{z}}, z)$, $\underline{\mathbf{z}} \in [0,1]^{D-1}$ is the projection of $\mathbf{z}$, and $z \in [0,1]$ is its last component, under the fractal distribution μ_D. Analogously let $\mathbf{x} = (\underline{\mathbf{x}}, x)$, where $\underline{\mathbf{x}} \in [0,1]^{D-1}$ and $x \in [0,1]$. Here $\mathbf{x}$ is given.

Then:

$$\begin{aligned}
U_D(r,\mathbf{x}) &= \int_0^r \frac{\partial U_1(\rho,x)}{\partial\rho} U_{D-1}(\sqrt{r^2-\rho^2},\underline{\mathbf{x}})d\rho\,,\\
&\geq \int_0^r \frac{\partial U_1(\rho,x)}{\partial\rho} U_{D-1}(\sqrt{r^2-\rho^2},\underline{0})d\rho\,,\\
&= U_D(r,(\underline{0},x))\\
&= \int_0^r \frac{\partial U_{D-1}(\rho,\underline{0})}{\partial\rho} U_1(\sqrt{r^2-\rho^2},x)d\rho\,,\\
&\geq \int_0^r \frac{\partial U_{D-1}(\rho,\underline{0})}{\partial\rho} U_1(\sqrt{r^2-\rho^2},0)d\rho\,,\\
&= U_D(r,0)\,.
\end{aligned}$$

□

Corollary 2. *The signal received at $\mathbf{x}=0$ is smaller in distribution than the signal received at any other point of $\mathcal{K}(a,\ell)^D$.*

Let us now prove theorem III.1 and III.2 for the fractal map $\mathcal{K}^2(a,\ell)$ but we conjecture that they hold for any fractal maps.

B. Proof of theorem III.1

First, an upper bound of the loss probability ρ_n is introduced.

Lemma 3.

$$\rho_n \leq n\mathbb{P}\left\{S_n(\lambda_n,0) < K\right\}\,. \tag{13}$$

Proof. Via a straightforward upper bound, the following is obtained:

$$\rho_n \leq \sum_{\mathbf{y}\in\mathcal{R}} \mathbb{P}\left\{S_n(\lambda_n,\mathbf{y}) < K\right\}\,. \tag{14}$$

For a given node $\mathbf{y}$ in $\mathcal{R}$:

$$\begin{aligned}
&\mathbb{P}\left\{S_n(\lambda_n,\mathbf{y}) < KN\right\}\\
&= \int_{[0,1]^2} \mu_2(\mathbf{z})\mathbb{P}\left\{S_n(\lambda_n,\mathbf{z}) < K\right\}\mathbb{P}\left\{\mathbf{y}=\mathbf{z}\right\}d\mathbf{z}^2
\end{aligned}$$

since $\mathbf{y}$ is distributed according to the measure μ_2 and thus

$$\rho_n \leq n\int_{[0,1]^2} \mu_2(\mathbf{z})\mathbb{P}\left\{S_n(\lambda_n,\mathbf{z}) < K\right\}d\mathbf{z}^2\,. \tag{15}$$

Since $S_n(\lambda_n,\mathbf{z}) \geq S_n(\lambda_n,0)$ in distribution thus $\mathbb{P}\left\{S_n(\lambda_n,\mathbf{z})\right\} \leq \mathbb{P}\left\{S_n(\lambda_n,0)\right\}$ thus $\rho_n \leq n\mathbb{P}\left\{S_n(\lambda_n,0) < KN\right\}$. □

Let us now prove a Chebyshev formula.

Lemma 4. *There exist $B_F, C_F > 0$ such that for all $\theta > 0$ the following bound exists:*

$$\log\mathbb{E}\left\{\exp(-\theta S_n(\lambda_n,0))\right\} \leq \lambda_n\left(-C_F(P_n\theta)^{\gamma_F} + B_F P_n\theta\right)\,, \tag{16}$$

with $\gamma_F = \frac{d_F}{2}$.

Proof. In a first stage it is assumed that no fading factor is present, *i.e.* $\mathbf{F}_{r,t}=1$ for all $(r,t)\in\mathcal{R}\times\mathcal{T}$. Referring to [13] and [6]:

$$\begin{aligned}
&\mathbb{E}\left\{\exp(-\theta S_n(\lambda_n,0))\right\}\\
&= \exp\left(-\lambda_n\int_{[0,1]^2}(1-e^{-P_n\theta\|\mathbf{z}\|^{-\alpha}})\mu_2(\mathbf{z})d\mathbf{z}^2\right)\,.
\end{aligned}$$

Clearly, since $\theta > 0$, we have

$$\begin{aligned}
&\mathbb{E}\left\{\exp(-\theta S_n(\lambda_n,0))\right\}\\
&= \exp(-\lambda_n\int_{(\mathbb{R}^+)^2}(1-e^{-\theta\|\mathbf{z}\|^{-\alpha}})\mu_2^*(\mathbf{z})d\mathbf{z}^2\\
&- \lambda_n\int_{(\mathbb{R}^+)^2\setminus[0,1])^2}(1-e^{-\theta\|\mathbf{z}\|^{-\alpha}})\mu_2^*(\mathbf{z})d\mathbf{z}^2),
\end{aligned} \tag{17}$$

where μ_2^* is the extension of measure μ_2 over the whole unbounded $\mathcal{K}^*(a,\ell)^2$.

The integral $\int_{(\mathbb{R}^+)^2}(1-e^{-\theta\|\mathbf{z}\|^{-\alpha}})\mu_2^*(\mathbf{z})d\mathbf{z}^2$ is the function $f(\theta,0)$ in [6] computed on the whole infinite Cantor map with $\alpha=2$. It is known that $f(\theta,0) = \theta^{\gamma_F}P(\log\theta)$, with $\gamma_F = \frac{d_F}{\alpha}$ and $P(\cdot)$ is a positive function which periodic with small oscillations. We can say that $f(\theta,0) \geq C\theta^{\gamma_F}$ for some constant $C>0$ and therefore $\lambda_n\int_{(\mathbb{R}^+)^2}(1-e^{-P_n\theta\|\mathbf{z}\|^{-\alpha}})\mu_2^*d\mathbf{z}^2 \geq \lambda_n C(P_n\theta)^{\gamma_F}$.

Let

$$J(\theta) = \int_{(\mathbb{R}^+)^2\setminus[0,1]^2}(1-e^{-\theta\|\mathbf{z}\|^{-\alpha}})\mu_2^*(\mathbf{z})d\mathbf{z}^2\,.$$

One can notice that if $\|\mathbf{z}\|\leq 1$ and $\mathbf{z}\in\mathcal{K}^*(a,\ell)^2$ then $\mathbf{z}\in\mathcal{K}(a,\ell)^2$. The following is obtained:

$$J(\theta) \leq \int_{\|\mathbf{z}\|\geq 1}(1-e^{-\theta\|\mathbf{z}\|^{-\alpha}})\mu_2^*(\mathbf{z})d\mathbf{z}^2$$

Rewritten as:

$$\begin{aligned}
&\int_{\|\mathbf{z}\|\geq 1}(1-e^{-\theta\|\mathbf{z}\|^{-\alpha}})\mu_2^*(\mathbf{z})d\mathbf{z}^2\\
&= \int_1^\infty (1-e^{-\theta r^{-\alpha}})\frac{\partial}{\partial r}U_2^*(r,0)dr\,,
\end{aligned} \tag{18}$$

where for $\mathbf{x}\in\mathcal{K}^*(a,\ell)$ and for real r

$$U_2^*(r,\mathbf{x}) = \int_{(\mathbb{R}^+)^2}\mathbb{I}\left(\|\mathbf{z}-\mathbf{x}\|\leq r\right)\mu_2^*(\mathbf{z})d\mathbf{z}^2\,. \tag{19}$$

Thus, using the inequality $1-e^{-x} \leq x$ and integration by parts an upper bound on $J(\theta)$ is achieved:

$$\begin{aligned} J(\theta) &\leq \theta \int_1^\infty r^{-\alpha} \frac{\partial}{\partial r} U_2^*(r,0) dr \\ &= \theta \left([U_2^*(r,0) r^{-\alpha}]_1^\infty + \alpha \int_1^\infty r^{-\alpha-1} U_2^*(r,0) dr \right) \\ &= -\theta U_D^*(1,0) + \theta\alpha \int_1^\infty r^{-\alpha-1} U_2^*(r,0) dr \\ &\leq \theta\alpha \int_1^\infty r^{-\alpha-1} U_2^*(r,0) dr \,. \end{aligned}$$

From [13], it is known that $U_D^*(r,0) = P_2(\log r) r^{d_F}$ where $P_2(.)$ is a non negative periodic function. Thus there exists $B^* > 0$ such that $W_2^*(r,0) \leq B^* r^{d_F}$, thus

$$J(\theta) \leq \frac{\alpha B^*}{\alpha - d_F} \theta = B\theta \,,$$

with the appropriate value for constant $B > 0$. Therefore

$$\mathbb{E}\left\{\exp(-\theta S_n(\lambda_n, 0)\right\} \leq \exp\left(-\lambda_n (C_F (P_n\theta)^{\gamma_F} - B_F P_n \theta\right).$$

This proves the lemma for the case with no fading ($\mathbf{F} = 1$). The case when the fading factor $\mathbf{F}$ is not identically equal to 1 is straightforward. In this case we know that

$$\begin{aligned} &\mathbb{E}\left\{\exp(-\theta S_n(\lambda_n, 0))\right\} = \\ &\exp\left(-\lambda_n \mathbb{E}\left\{ \int_{[0,1]^2} (1 - e^{-\mathbf{F} P_n \theta \|\mathbf{z}\|^{-\alpha}}) \mu_2(\mathbf{z}) d\mathbf{z}^2 \right\} \right) \end{aligned} \quad (20)$$

thus

$$\begin{aligned} &\mathbb{E}\left\{\exp(-\theta S_n(\lambda_n, 0))\right\} \\ &\leq \exp\left(\mathbb{E}\left\{\lambda_n (-C_F (\mathbf{F} P_n \theta)^{\gamma} + B_F \mathbf{F} P_n \theta\right\}\right) \\ &= \exp\left(\lambda_n (-C_F \mathbb{E}\left\{\mathbf{F}^{\gamma}\right\} P_n \theta + B_F P_n \theta)\right) \,, \end{aligned}$$

since $\mathbb{E}\left\{\mathbf{F}\right\} = 1$.

□

End of proof of theorem III.1. Via the Chebyshev inequality we have

$$\rho_n \leq n \exp\left(-\lambda_n (C_F (P_n\theta)^{\gamma_F} - B_F P_n \theta) + K\theta\right) . \quad (21)$$

The idea is to find the value of θ which minimizes the right-hand side of (21). This is equivalent to minimizing

$$\lambda_n \left(-C_F \tau_n^{\gamma_F} + A_n \tau_n\right) , \quad (22)$$

obtained by exchanging θ with $\tau_n := P_n\theta$ and introducing $A_n = B_F + K/E_n$, which is achieved at

$$\tau_n = \left(\frac{A_n}{\gamma_F C_F} \right)^{\frac{1}{\gamma_F - 1}} . \quad (23)$$

Then the minimal value of (22) is given by

$$-\left(C_F \gamma_F\right)^{\frac{1}{1-\gamma_F}} \left(\frac{1}{\gamma_F} - 1 \right) \lambda_n A_n^{\gamma_F/(\gamma_F - 1)} . \quad (24)$$

Thus ρ_n tends to 0 when

$$\log n - \left(C_F \gamma_F\right)^{\frac{1}{1-\gamma_F}} \left(\frac{1}{\gamma_F} - 1 \right) \lambda_n A_n^{\gamma_F/(\gamma_F - 1)} \to -\infty \,. \quad (25)$$

Notice that $E_n \to 0$ is equivalent to $A_n \to \infty$, hence: $A_n / \left(\frac{K}{E_n}\right) \to 1$.

Then $\rho_n \to 0$, i.e. (25) is satisfied, if

$$\log n = o\left(\lambda_n E_n^{\gamma_F/(1-\gamma_F)}\right) . \quad (26)$$

□

As a concrete example of this result, we stated the Corollary 1, $E_n = \omega\left(\left(\frac{\log n}{n}\right)^{\frac{1-\gamma_F}{\gamma_F}}\right)$. As a matter of fact if the fractal map is $\mathcal{K}(\frac{1}{8}, 4)$ we have $d_F = \frac{4}{3}$, then $\gamma_F = \frac{2}{3}$ and $E_n = O(n^{-1/2})$ when $\lambda_n = \beta n$ with $n \to \infty$.

C. Proof of theorem III.2

Let us start with the following lemma

Lemma 5. *Considering $d_{\min} > 0$, there exists D_F such that for all $d_{\min} \geq 0$ and for all $\theta > 0$ the following bound holds:*

$$\begin{aligned} &\log \mathbb{E}\left\{\exp(-\theta S_n(\lambda_n, 0))\right\} \\ &\leq \lambda_n \left(-C_F (P_n\theta)^{\gamma_F} + B_F P_n \theta + D_F d_{\min}^{d_F} \right) \end{aligned} \quad (27)$$

Proof. With the modification that: $S(\lambda_n, \mathbf{x}) = \sum_{\mathbf{z} \in \mathcal{T}} \mathbf{F}(\mathbf{x}, \mathbf{z}) \left(\max\{d_{\min}, \|\mathbf{z} - \mathbf{x}\|\}\right)^{-2}$ we still have $S(\lambda_n, \mathbf{x}) \geq S(\lambda_n, 0)$ in distribution. To simplify, it is assumed $\mathbf{F} = 1$, the case $\mathbf{F}$ not identically equal to 1 will be easy to handle as previously done. Now one gets

$$\begin{aligned} f(\theta, 0) &= \int_{[0,1]^2} (1 - e^{\theta \|\mathbf{z}\|^{-2}}) \mu_2(\mathbf{z}) d\mathbf{z}^2 \\ &\quad - \int_{\|\mathbf{z}\| \leq d_{\min}} \left(e^{-\theta d_{\min}^{-2}} - e^{\theta \|\mathbf{z}\|^{-2}}) \right) \mu_2(\mathbf{z}) d\mathbf{z}^2 . \end{aligned}$$

The second term of the right hand side term can be lower bounded by $U_2(d_{\min}, 0)$. In fact it is as if we assumed that in the worst case the receiver does not receive zero energy from a transmitter when the antenna aperture overlap. Using the bound $U_2(r,0) \leq D_F r^{d_F}$ one gets the bound:

$$f(\theta, 0) \geq C_F \theta^{\gamma_F} - B_F \theta - D_F d_{\min}^{d_F} . \quad (28)$$

□

End of proof of theorem III.2. We still have the Chebyshev inequality but it now reads:

$$\rho_n \leq n \exp\left(-\lambda_n (C_F (P_n\theta)^{\gamma_F} - B_F P_n \theta - D_F d_{\min}^{d_F}) + K\theta \right) \quad (29)$$

Still with $\tau_n = P_n\theta$, the following quantity has to be minimized:

$$\lambda_n (-C_F \tau_n^{\gamma_F} + A_n \tau_n + D_F d_{\min}^{d_F}), \quad (30)$$

with $A_n = B_F + K/E_n$. The opimal is attained for

$$\tau_n = \left(\frac{A_n}{\gamma_F C_F} \right)^{\frac{1}{\gamma_F - 1}} . \quad (31)$$

which gives the minimal value of (30):

$$-\lambda_n \left((C_F \gamma_F)^{\frac{1}{1-\gamma_F}} \left(\frac{1}{\gamma_F} - 1 \right) A_n^{\gamma_F/(\gamma_F-1)} - D_F d_{\min}^{d_F} \right). \quad (32)$$

Clearly there is $A_F > 0$ such that if $A_n = A_F d_{\min}^{(\gamma_F-1)d_F/\gamma_F} = A_F d_{\min}^{(\gamma_F-1)/2}$ then $\rho_n \to 0$. This is equivalent to having:

$\limsup_{n\to\infty} E_n = E_{\min}$ of order $d_{\min}^{(1-\gamma_F)/2}$ which tends to 0 when $d_{\min} \to 0$.

□

V. Numerical experiments

We first conduct simulations in a fractal map of $\mathcal{K}^2(1/8, 4)$, where positions of the transmitters and receivers are obtained as a Poisson shot. We keep the numbers of transmitters receivers equal, denoted by $\lambda_n = n$, and vary $n = 100, 200, 300, \ldots, 5700$. The SNR threshold for a successful packet reception is first taken for $K = 1$dB and path loss coefficient $\alpha = 2$. Then simulations are conducted for four relevant values of $d_{min} = 0, \quad 0.02, \quad 0.04$ and $d_{min} = 0.1$, where we assume negligible antenna cross section.

Figure 3 displays the the results obtained for the total energy required for $\rho = 0$, $SNR = 1$dB in a fractal map $\mathcal{K}^2(1/8, 4)$. The simulation results validate that the energy required to ensure the capture condition decreases with d_{min}, attaining the minimum values for $d_{min} = 0$.

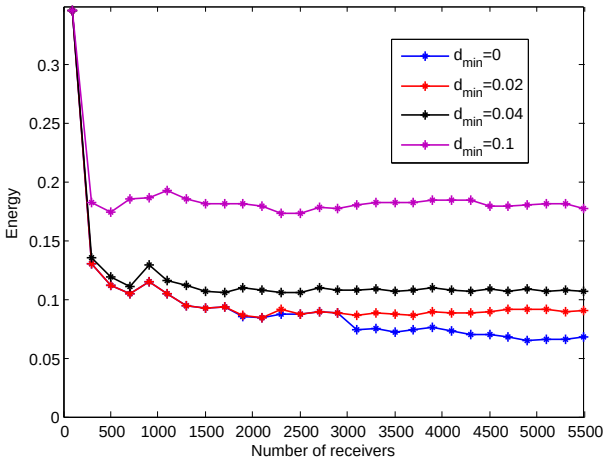

Figure 3: Variation of total energy in fractal maps of $\mathcal{K}^2(1/8, 4)$, SNR threshold $K = 1$dB, $\alpha = 2$

In order to show that the decrease in energy is a property specific to networks in fractal maps, we run the experiments with the same set of parameters in a uniform Poisson map that can be expressed as $K^2(\frac{1}{l}, l)$.

Figure 4 displays the results obtained for the total energy required in order to ensure probability of packet loss equal to zero in a uniform map. In this scenario also E_n is smaller for smaller values of d_{min}. Although we can observe a minor decrease in the total energy when the density of the nodes increases, the savings of energy are not as large as in fractal maps. To the contrary, the plots show rather a constant

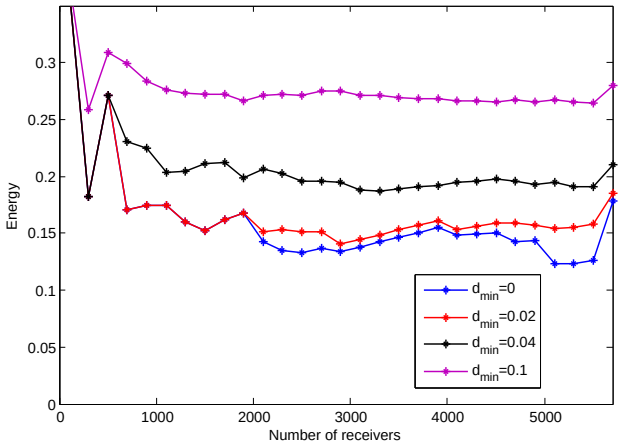

Figure 4: Variation of total energy in a uniform Poisson map, SNR threshold $K = 1$dB, $\alpha = 2$

behavior in the energy consumption as the number of nodes varies. Furthermore, importantly, E_{min} in a fractal map is always inferior to the total energy in the uniform Poisson map. Let us validate this through an additional experiment.

For further demonstrating that the results obtained in fractal maps are superior to the ones in uniform maps, we run simulations for several values of SNR, for the same value of $d_{min} = 0$. Figure 5 shows the energy obtained in fractal map $\mathcal{K}^2(1/8, 4)$ versus the one in uniform maps for the SNR $K = 1, 3, 5$ dB. In every scenario, the energy required to ensure zero loss probability under SNR threshold K is higher in uniform maps. Furthermore, a closer look at the interval

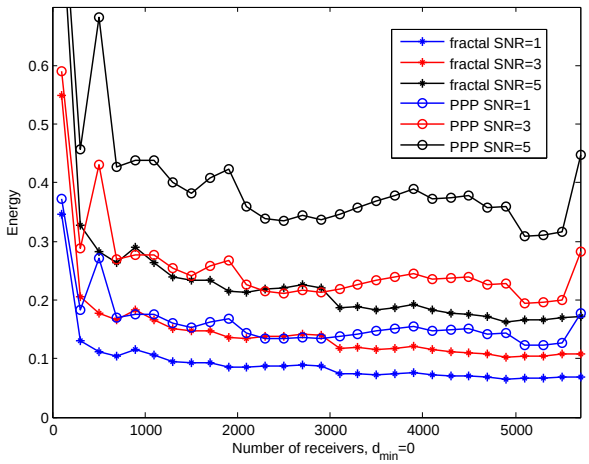

Figure 5: Results for energy in fractal maps $\mathcal{K}^2(1/8, 4)$ and uniform maps for different values of SNR, $\alpha = 2$

of points 2000 to 3000 for SNR $K = 3$dB in fractal maps shows that the same results are obtained for $K = 1$ dB in uniform Poisson map. This is a promising result and provides the intuition that by using the same level of energy in a fractal map, one could obtain a superior quality of transmission.

In fact, Figure 6 shows that the energy necessary for SNR capture decreases with the decrease of a, and therefore with the decrease of the fractal dimension. Notice how for $a = 0.02$, the energy approaches the zero limit for lower values of the number of receivers.

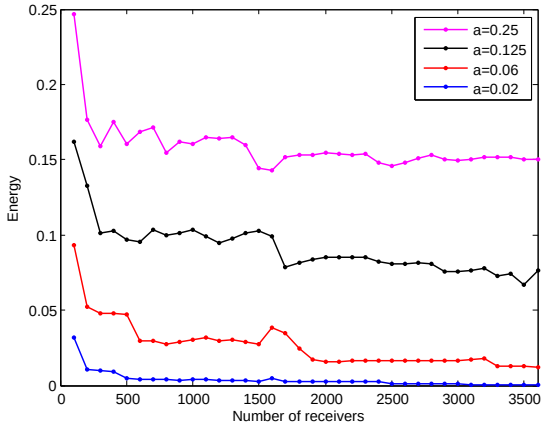

Figure 6: Simulated energy in fractal maps $\mathcal{K}^2(a, 4)$ for different values of a

Next, we validate Corollary 1, $E_n = \omega\left(\left(\frac{\log n}{n}\right)^{\frac{1-\gamma_F}{\gamma_F}}\right)$. Figure 7 shows the energy obtained through simulations versus the scaling law for $a = 1/8$ and $l = 4$. For this values, the law reads as $n^{-1/2}$.

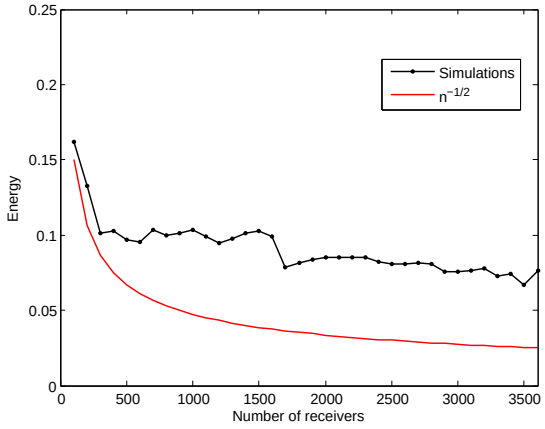

Figure 7: Simulated energy in fractal map $\mathcal{K}^2(1/8, 4)$, SNR threshold $K = 1$dB versus $n^{-1/2}$, $\alpha = 2$

VI. Conclusion

This paper brings into consideration a surprising fact: the energy needed to transmit a packet tends to zero when the number of receivers increases. We proved, theoretically and experimentally, that in a Poisson shot in a fractal map support, the total energy required for a zero loss probability in a virtual MISO setup decreases with the increase of the populations. Moreover, the phenomenon does not reproduce under a uniform distribution of the devices, making it a unique property of the networks of devices distributed in a Cantor map. The setup offers an evident energy saving comparing to the conventional setups based on a Poisson Point Process.

VII. Discussion

In this work we have assumed that: one can neglect the antenna cross section, the density of nodes is overwhelming, and the path loss coefficient is 2. These assumptions may be claimed not to be realistic, and one may argue about the validity of the results. Our results indicate that savings in the energy consumption may occur even under more realistic values for the path loss exponent and distance between sensors. To prove this phenomena remains as a subject of our future work. Finally, this work opens up new horizons for studying fractal sensor networks.

References

[1] P. Gupta and P. R. Kumar, "The capacity of wireless networks," *IEEE Trans. Inf. Theor.*, vol. 46, pp. 388–404, Sept. 2006.

[2] M. Haenggi, J. G. Andrews, F. Baccelli, O. Dousse, and M. Franceschetti, "Stochastic geometry and random graphs for the analysis and design of wireless networks," *IEEE Journal on Selected Areas in Communications*, vol. 27, pp. 1029–1046, September 2009.

[3] F. Baccelli, B. Blaszczyszyn, and P. Muhlethaler, "An aloha protocol for multihop mobile wireless networks," *IEEE Transactions on Information Theory*, vol. 52, pp. 421–436, Feb 2006.

[4] S. Malik and P. Jacquet, "Optimizing local capacity of wireless ad hoc networks," in *2011 4th Joint IFIP Wireless and Mobile Networking Conference (WMNC 2011)*, pp. 1–8, Oct 2011.

[5] N. Deng, W. Zhou, and M. Haenggi, "The ginibre point process as a model for wireless networks with repulsion," *IEEE Transactions on Wireless Communications*, vol. 14, pp. 107–121, Jan 2015.

[6] P. Jacquet, "Optimized outage capacity in random wireless networks in uniform and fractal maps," in *IEEE International Symposium on Information Theory, ISIT 2015, Hong Kong, China, June 14-19, 2015*, pp. 166–170, IEEE, 2015.

[7] M. Batty and P. Longley, *Fractal Cities: A Geometry of Form and Function*. San Diego, CA, USA: Academic Press Professional, Inc., 1994.

[8] Wikipedia, "Near and far field — wikipedia, the free encyclopedia," 2017.

[9] J. Zhao, "The absence of isolated node in geometric random graphs," in *2015 53rd Annual Allerton Conference on Communication, Control, and Computing (Allerton)*, pp. 881–886, Sept 2015.

[10] C. Florens and R. McEliece, "Packets distribution algorithms for sensor networks," in *IEEE INFOCOM 2003*, vol. 2, pp. 1063–1072 vol.2, March 2003.

[11] S. Shakkottai, R. Srikant, and N. Shroff, "Unreliable sensor grids: coverage, connectivity and diameter," in *IEEE INFOCOM 2003*, vol. 2, pp. 1073–1083 vol.2, March 2003.

[12] H. Ding, C. Xing, S. Ma, G. Yang, and Z. Fei, "Transmission capacity of clustered ad hoc networks with virtual antenna array," *IEEE Transactions on Vehicular Technology*, vol. 65, pp. 6926–6939, Sept 2016.

[13] P. Jacquet, "Capacity of simple multiple-input-single-output wireless networks over uniform or fractal maps," in *2013 IEEE 21st International Symposium on Modelling, Analysis and Simulation of Computer and Telecommunication Systems, San Francisco, CA, USA, August 14-16, 2013*, pp. 444–453, IEEE Computer Society, 2013.

[14] J. Li and P. Mohapatra, "An analytical model for the energy hole problem in many-to-one sensor networks," in *VTC-2005-Fall. 2005 IEEE 62nd Vehicular Technology Conference, 2005.*, vol. 4, pp. 2721–2725, Sept 2005.

[15] H. T. Friis, "A note on a simple transmission formula," *Proceedings of the IRE*, vol. 34, pp. 254–256, May 1946.